Direct Electrolysis of Lithium on Copper

by

Gayatri Pode

A Thesis Presented in Partial Fulfillment
of the Requirements for the Degree
Master of Science

Approved April 2019 by the
Graduate Supervisory Committee:

Nathan Newman, Chair
Daniel Marshall
Meng Tao

ARIZONA STATE UNIVERSITY

May 2019

ABSTRACT

Lithium metal is a promising anode for the next generation lithium batteries owing to its high capacity (3860 mAh g^{-1}) and the lowest negative reduction potential (-3.04 V). Commercial produced lithium anodes have a native rough surface which deteriorates the cycling performance of the battery. Here, an attempt has been made to deposit lithium on copper from an electrolytic cell consisting of simple electrolyte of pyridine and lithium chloride at room temperature. Water is known to react aggressively with the lithium metal, however in the electrochemical plating process, it has a significant beneficial effect in catalyzing the electrochemical reactions. The effect of trace amounts of water was investigated in air as well as in controlled atmosphere of argon, nitrogen, breathing grade dry air and ultra-zero dry air. The electrochemical products examined by Fourier transform infrared spectroscopy revealed the deposition might require the reduction of pyridine to facilitate the reduction of the lithium salt. Purity of the lithium film was determined by inductively coupled plasma mass spectrometry.

ACKNOWLEDGEMENTS

I would first like to thank my principal investigator, Dr. Nathan Newman for giving me the opportunity to work in his laboratory. The state-of-the-art facilities at the Newman Research Group made this thesis successful. His consistent encouragement and advise proved to be very valuable throughout this work.

I express my heartfelt thanks to my research advisor, Dr. Daniel Marshall for his immense knowledge, motivation, everlasting support, enthusiasm and patience. His thoughtful insights, creativity and unique way of tackling problems has guided me throughout my master's program. His acquaintance is key factor for my improved personality.

I am also very grateful to Dr. Meng Tao for his technical advice and willingness to serve on my defense committee. He always patiently answered all my queries and steered me in the right direction. I value his suggestions and corrections towards my thesis.

I acknowledge the use of facilities within the Goldwater Materials Science Facility, Machine and Electrical Shop, Glass Blowing facility and Keck Laboratory. I would like to thank Emmanuel Soignard and David Wright for providing me with the correct resources and also Trevor Martin for extensively helping me with the mass spectrometry. I also want to thank Dr. Rakesh K. Singh for first introducing me to this research group. I extend my thanks to all the kind people around me – Mr. Richard Hanley, Mr. Cameron Kopas, Mr. Siddhesh Gajare, Mr. Justin Gonzales, Mr. Greg Vetaw, Mr. Guven Turgut, Mr. Madhu Krishna Murthy, Mr. Ashwin Agathya Boochakravarthy, Mr. Dheepak Surya Kalyana Raman, Mr. Chris Gregory, Mr. Elias Sugarman, Mr. Bryan Ibarra Mercado and other members of the group for their immense support and friendship.

TABLE OF CONTENTS

Page

CHAPTER Page

LIST OF TABLES

Table Page

LIST OF FIGURES

Figure Page

CHAPTER 1

INTRODUCTION

1.1 Overview

According to the US Geological Survey, Mineral Commodity Summaries January 2018 issue, worldwide lithium production has been elevated by 13 % to 43,000 tons in 2017 owing to the dramatic growth of lithium battery technology and electric vehicle manufacturers. Although the lithium markets observe variation as per the location, the estimation is as follows: Batteries: 46 %, ceramics and glass: 27 %, lubricating grease:7 %, continuous casting mold flux powders: 4 % and various industrial uses like air treatment, polymer production and other uses approximate at around 5 % each [1]. Lithium metal has always been the holy grail of the battery storage industry. Paul et al. has discussed the current state of research of lithium metal batteries and is positive about the transition of

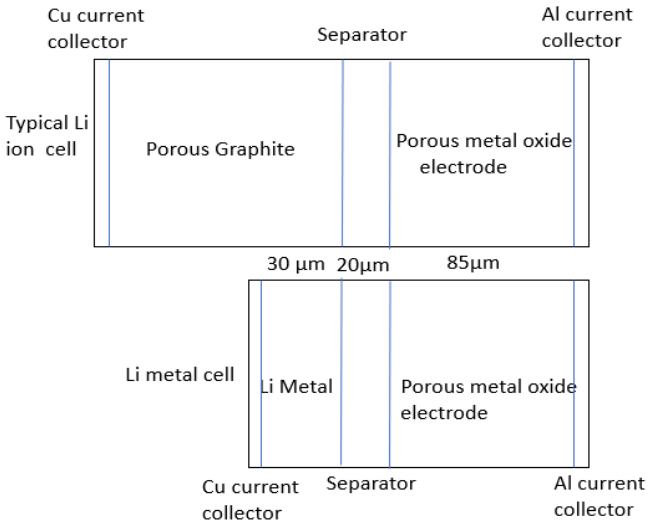

Figure 1. Schematic Comparison of Lithium Ion and Lithium Metal Cell

Lithium Ion Batteries to Lithium Metal Batteries (LMB) with higher energy density and low cost [2]. This is possible because lithium metal is the lightest of the very electropositive

metals and offers a specific coulombic capacity of 3860 mAh/g which is ten times greater than the standard graphite anode in lithium ion batteries. And there is reduction in the dead weight of the cell such as binders and host materials. But the challenge rises because of the lithium metal reactivity with the electrolyte, leading to volume expansion and dendrite formation. The dendrites have a dendritic-like appearance which grows on the lithium metal anode. During cycling with high currents, these lithium dendritic like structures can reach the cathode causing short circuit of the battery. Figure 1 shows a simple schematic that describes how the battery dimensions affect the density of cell packing, hence leading to higher energy density and capacity. The success and issues of this transition along with the diversified history of batteries that have evolved during the past decades is reported in [3].

Lithium is a soft, shiny and highly reactive metal with low melting point of 180 C, on reaction it leads to release of huge quantities of heat and often hazardous products. The reactivity increases with surface area and temperature. It is air sensitive and reacts violently with water releasing flammable hydrogen gas. It is incompatible with acids and oxidizers. Nitrogen gas reacts with lithium metal at room temperature to form a hygroscopic layer of Li_3N.

Health hazards of exposure to lithium includes irritation to the eyes, skin and it is corrosive on ingestion. Special precautions are thereby taken; all the lithium handling is performed in a dry environment, mostly in a glove box with inert argon atmosphere. Lithium metal is packaged in an airtight container, sealed with argon gas, stored under mineral oil or beneath a layer of petroleum jelly or paraffin wax. Exposure to atmospheric conditions can cause significant contamination of lithium surfaces as well as structural and hence electrical

inhomogeneity. In lithium metal batteries, the major failure mechanism is the formation of lithium dendrites which narrows down the lifetime of battery due to the uneven and localized deposition of lithium during the plating/stripping cycles. These dendrites nucleate to the surface and can short the battery. There is a clear need to produce high purity lithium with better control over the microstructure to suppress the unwanted reactions with the electrolytes.

1.2 Background

Lithium is primarily extracted from various brines with significant amounts of lithium, and pegmatite ores which is recovered as spodumene mineral. The lithium extraction involves chemical precipitation, adsorption, solvent extraction and membrane exchange technology. The yield obtained is mostly in the form of lithium carbonate or lithium hydroxide and one of these is used as feedstock for producing lithium metal or other lithium compounds. Converting lithium into metallic form is done by the electrolysis of eutectic LiCl-KCl (55%-45 %) salt at around 500 C. The typical cell is a steel container with a refractory lining to maintain the salts at high temperature. Submerged steel electrodes act as the cathode During electrolysis the lithium metal rises on the surface of the melt. Chlorine gas released at the graphite anodes may create problems when in contact with this newly formed lithium, hence it has to constantly skimmed and poured out [4]. Pure lithium metal products include forms of bulk, ingot, rod, wires, foil, pellets and stabilized lithium metal powder with purity range from 99 % to 99.9 %. With a view to maintain low production costs and high throughputs, preferred routes for making lithium anodes are mechanical pressing, rolling, foil processing with extrusion and calendaring, spin coating and vacuum deposition, depending on the thickness and shape required. The most common form used

in battery applications is lithium metal foil. Electrodeposition of lithium is quite rare because it is primarily used to study the battery plating/stripping cycles. In 1899, it was found that metallic lithium can be electrodeposited at room temperature from solutions of lithium chloride in pyridine [5]. Some investigations were further made by Mott and Pattern studying the decomposition curves of LiCl in pyridine, acetone and alcohols [6,7]. In their study after a period, the high voltages used, decomposed the electrolyte and turned the electrolyte brown and hence were not recommended for high volume manufacturing. Turning the lithium metal ingot into foils produced from the conventional route of electrolysis of LiCl – KCl eutectic involved high temperatures plus additional mechanical processing. In controlled atmosphere, to have lithium foils in the micrometer range at room temperature with a simpler assembly was a challenge. A concept of a "lithium free" thin film battery; in situ fabrication of lithium anode had then gained momentum. Prior to the deposition, it is basically a lithium ion battery in a discharged state. Following this, BJ Neudecker et al. examined a cell structure of Cu/solid lithium electrolyte (LiPON)/LCO. The typical charging cycle was for 15 mins at 4.2 V with a current density of 1 $\mu A/cm^2$ and it gave a thickness of 0.7 μm. But the performance of such cells decreased dramatically after only 100 cycles [8]. Advances were made in this concept; owing to greater conductivity and wettability of liquid electrolytes, there was a shift to highly concentrated ether solvents and LiFSI enabling high cycling rate of Li anode with better columbic efficiency up to 99.1 % [9]. But for these, extra precautions had to be taken to reduce the reactions between the plated Li and the electrolyte. An alternative technique to deposit lithium using the standard battery electrolyte – carbonates plus $LiPF_6$ salt, was to use lithium metal foil as a source of lithium ions instead of the battery cathode material. The

electrodeposited lithium film when used as an anode in a coin cell gave similar electrochemical performance to lithium bulk metal anodes [10]. Yet another room temperature electrolytic deposition of Li on copper anode used lithium(selective) ion conducting (LIC) layer that carried lithium ions from lithium carbonate or any other salt that would dissociate in an acid to organic conducting electrolyte. The purity obtained was as high as 99.985 wt % and the morphology could be tuned depending on the current density; 1 – 10 mAmp/cm^2 [11]. The assembly had some formation of chemical gases whose nature hasn't been studied yet and the expensive LIC decomposes after time.

To improve the surface chemistry of pristine lithium, an easy way of chemical polishing with naphthalene has been demonstrated to improve the electrochemical performance of LMBs [12].

1.3 Objective

The purpose of this work is to find out a much easier fabrication and less expensive technique to deposit lithium and characterize the deposited film. The motivation is to generate lithium ions directly from the salts to the solid electrode without a) melting of the lithium salts (i.e. no use of high temperature processing), or b) lithium ion conducting ceramic layer. It will help avoid root cause of higher production costs - complexity, time consuming assemblies and to eliminate the need for any additional pre/post treatment polishing steps. Readily available materials are to be chosen that can be used to attain pristine lithium film by direct electrolysis. The film purity is characterized using by Inductively Coupled Plasma Mass Spectrometry (ICP MS). The electrochemical products are studied by Fourier Transform Infrared Spectroscopy (FTIR).

CHAPTER 2

EXPERIMENTAL

2.1 Materials

The assembly set up consists of anode, cathode, electrolyte and dc power supply in a clean fume hood and glove box.

The anode is the positive electrode comprised of mesh styled platinized on titanium with dimensions 1" X 4" X 0.1" with a 3" tap. Superior electrical conductivity copper with purity 99.99% (McMaster-Carr) was used as the negative electrode cathode. 12" X 12" X 0.0200" copper sheet was then cut into plates of 3.54" X 0.31".

The electrolytic cell relies on the electrolyte. Amongst all the solvents, the prospective solvents for the electrolyte should a) dissolve the lithium ion salts, b) be a conducting solution c) moderate interactions while not reacting with the lithium film formed. Pyridine is a weak Lewis base with density and viscosity same as water and has comparatively low vapor pressure at room temperature with a pungent odor.

Table 1. Physical Properties of Pyridine

Molecular weight	79.1
Density at 30 C	0.973 g/ml
Melting point	- 41.8 C
Boiling point	115.6 C
Electrical conductivity at 25 C	4.8×10^{-8} ohm^{-1}
Dielectric constant at 25 C	12.3
Vapor pressure at 13.2 C	10 mm Hg
at 57.8 C	100 mm Hg

Pyridine is an aromatic hydrocarbon with an active nitrogen having an unshared pair of electrons. This forms many metal pyridine complexes in the process of electrolysis.

Anhydrous Pyridine (99.8 % from Sigma Aldrich) was used. First solute tested was lithium chloride (Sigma Aldrich, ACS reagent ≥99 %). To further reduce the high voltages used and increase conductivity, the typical salt in the battery electrolyte – lithium tetrafluoroborate (Alfa Aesar, 98 %) was investigated. These materials are readily available and not expensive, satisfying the requirements of a simple, less expensive electrodeposition technique (figure 2).

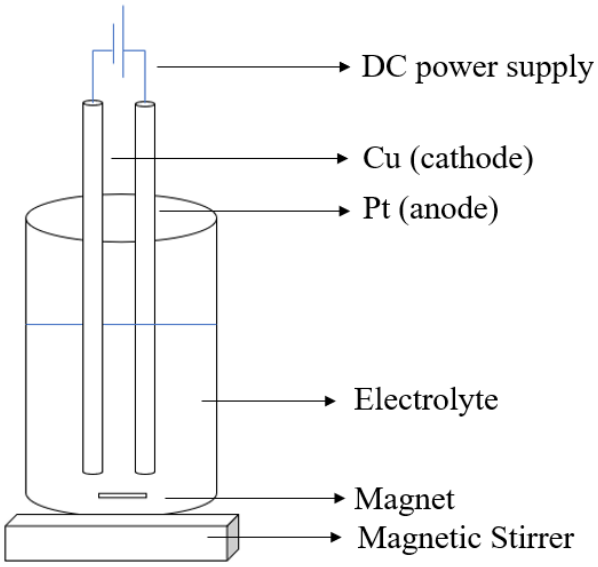

Figure 2. Schematic Two-Dimensional Representation of the Electrolytic Cell

The electrolytic cell was of glass with parallel platinum and copper electrodes maintained approximately 8 mm apart. The area of the copper immersed was between 2 and 2.5 cm^2. 100 ml pyridine was the standard amount of pyridine used for each deposition and this was just about enough to dissolve 1.32 grams of lithium chloride. The concentration used throughout this work was kept near the saturation limit - 1.5 grams/100 ml pyridine or 0.333 molar solution.

2.2 Methodology

2.2.1 Inductively Coupled Plasma Mass Spectrometry (ICP MS)

ICP MS is an analytical technique for quantitative elemental determination (metals as low as one part in billion, ppb) commonly used by many laboratories. It is simply a mass spectrometer with high temperature plasma source which converts the atoms of elements in the sample to ions. These ions are then separated by their mass to charge ratio and detected.

Sample introduction is done with a nebulizer which converts the liquid into aerosol further sweeping into the plasma to make ions. The plasma is made by partial ionization of the argon gas and the energy to generate this is obtained by applying an alternating current surrounding the gas. The plasma is sustained by a torch made up of quartz concentric tubes. The torch end is kept inside an RF induction coil. Argon flows through this torch and the electric spark introduces electrons into the gas stream. Interacting with the magnetic field of induction coil, these electrons accelerate in one direction first and change their direction with respect to the current. Collision with the argon atoms leads to release of new electrons which in turn get accelerated by the changing magnetic field. This process is maintained until the rate of new electrons released from the collisions is balanced by the rate of combining of electrons with Ar ions. At the end, it is mostly Ar atoms with small portion of free electrons and Ar ions. The elemental ions formed by the ICP discharge are typically positive – M^+ or M^{2+}, which are then driven into the mass spectrometer via the interface cone (sampler ~ 1 mm hole & skimmer ~ 0.4 mm hole). As from figure 3, intermediate vacuum is created so that the ions from the argon atmosphere (1-2 atm) are transmitted in to the low-pressure region (10^{-5} torr) of the mass spectrometer. The shadow mask helps to

prevent the photons (a light source), energy neutral and solid particles entering from the torch into the spectrometer.

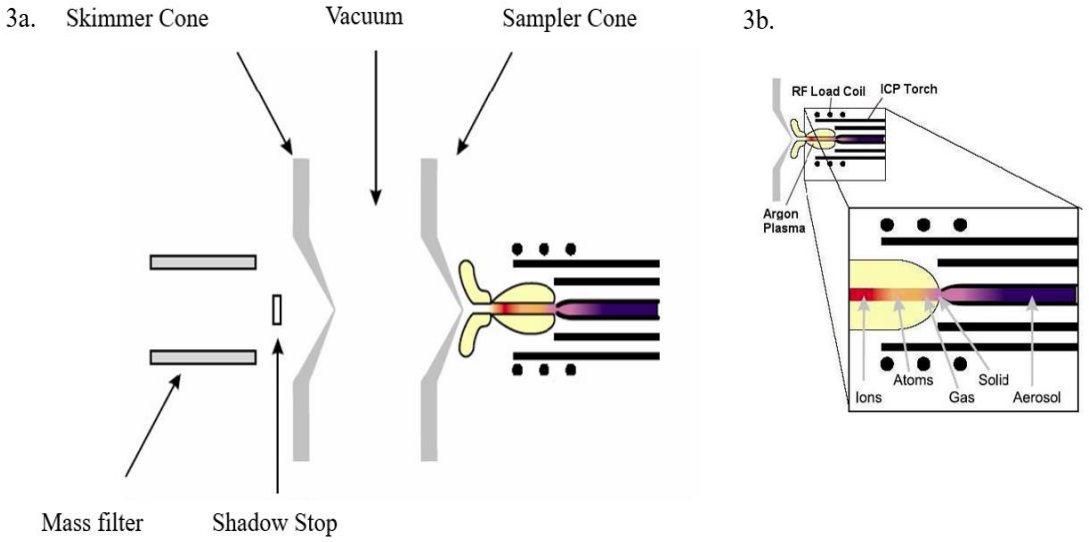

Figure 3a. Interface Region of the ICP MS & 3b. ICP Torch View in Detail[13]

The electrostatic lenses which has a positive charge serves as a collimator for the positively charged ions coming out of the ICP torch and hence focus it directly at the entrance of mass spectrometer. The ions entering the spectrometer are separated by their mass to charge ratio. Quadrupole mass filters are the most commonly used type, and work by setting AC and DC voltages to opposite pairs of rods. These voltages are rapidly switched which allows the ions of given (limited) mass to charge ratio remain stable and pass through the detector. These ions strike the detector and generate an electronic signal.

For sample preparation, the electroplated lithium film was first dissolved in ultra-high pure water and then were acidified with 2 % nitric acid using concentrated trace metal grade nitric acid. Samples were shaken well. Samples were analyzed using the Thermo Scientific iCAP-Q Quadrupole Inductively Coupled Plasma Mass Spectrometer using the instrument's Standard mode for the light elements (Li, Be, and B) while using the

instrument's Kinetic Energy Discrimination mode (KED) with ultra-high purity He collision gas for all remaining elements of interest.

2.2.2 Fourier Transform Infrared Spectroscopy (FTIR)

Fourier Transform Infrared Spectroscopy is used to identify chemical properties of organic, polymeric or, in some cases, inorganic materials by scanning the sample with infrared light. Infrared radiation of 10 to 12000 cm^{-1} is passed through the sample, the radiation energy is absorbed by the excitation of gets converted to the vibrational or rotational energy of the sample molecules. This signal is then perceived by the detector and presented as a spectrum. FTIR consists of a source, interferometer - beam splitter and a collector. From the source, a collimated light in IR range hits the interferometer which splits into two beams so that their paths are in two directions at different angles. One of them drives to the stationary mirror, other one goes to the moving mirror and both meet back at the beam splitter. The moving mirror motion creates a path length variation against the stationary mirror. The recombination thus produces constructive and destructive interreference.

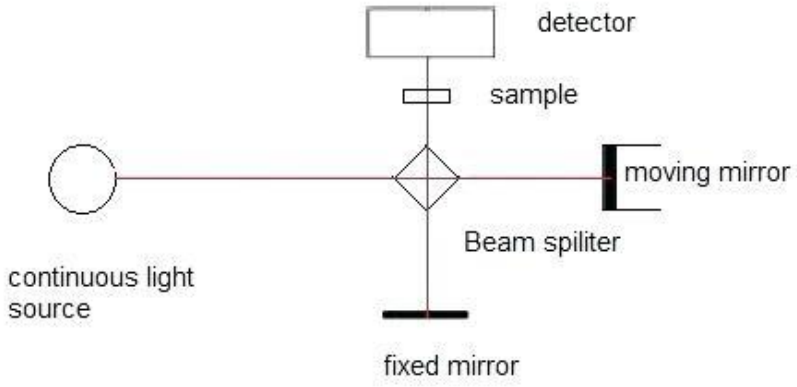

Figure 4. Block Diagram of FTIR[14]

The recombined beam is incident on the sample and the specific characteristic wavelengths are absorbed by the sample. The remaining reflected or transmitted beam is then detected as a function of wavelength. The instrument used was a Bruker IR spectrometer in ATR (attenuated total reflectance) mode. It works in a vacuum environment (4 – 5 mbar) The spectral range coverage is from 400 to 5500 cm^{-1}. The data was acquired with a sample scan of 32 and resolution 4 cm^{-1}. For liquid samples, a demountable liquid cell assembly was used that included a Teflon base plate, viton gasket, and Teflon holder.

5a 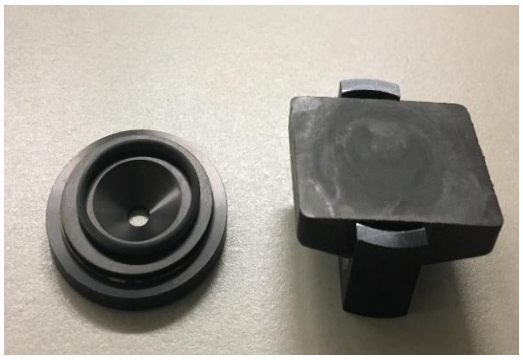 5b 

Figure 5a. Demountable Liquid Cell Assembly & 5b. Liquid Cell Assembled on FTIR

CHAPTER 3

RESULTS & DISCUSSIONS

3.1 Electrolysis in Atmospheric Fume Hood

First the electrolysis was carried out in a standard fume hood in atmosphere at 13-14 V and a shiny film deposition was seen. The current density as a function of time had an increasing trend.

Table 2. Electrolysis Parameters of One Third Molar LiCl in Pyridine at Room Temperature

Voltage (V)	**Current Density (mAmp/cm^2)**	**Time**	**Comment**
13	0.9729	Start	Shiny film formation
13	1.2567	30 sec	
14	1.3918	35 sec	Sudden increase in current
14	2.0135	5 mins	
14	2.2972	10 mins	
14	2.3783	15 mins	At this point addition of 1 gm of LiCl
14	2.6891	15.5 mins	
14	2.9054	20 mins	Black impurities seen, solution turned yellow

Secondary reactions were suspected due to

a) Continuous increasing current values
b) The turning black of the lithium film and the electrolyte changing its color to yellowish brown within 15-20 mins of electroplating

Similar results were found by Mott and Pattern [5] while studying the effect of water on electrolysis. Their assembly was isolated from the atmosphere by using a ground glass stopper. Water assisted the deposition, giving quicker discharge voltages thereby

increasing the deposition rate at which the preferred ions were deposited on the electrode. It also helps in the growth of insulating black film on the cathode. There was no comment in their paper on how water affected the electrochemical reactions and also there is uncertainty as to how effectively the reaction was isolated from the air with the ground glass stopper used. Since lithium is so reactive, working on lithium is expected to be done in an inert glove box atmosphere.

3.2 Electrolysis in a Glove Box

An attempt to first use an inexpensive glove bag was made. Under similar conditions as above, plating was seen, and the observations were no different. Argon was filled in the glove bag with a pressure at around 5 psi. Since intact evacuation from the surrounding air was not guaranteed, no conclusions could be made from this experiment.

Predicting the reaction would yield better current results for a longer period when carried out in a glove box proved to be inaccurate. The setup was shifted to argon glove box with completely new set of chemicals– lithium chloride and pyridine (not exposed to air). Unlike before, no plating was seen in-spite of increasing the voltage or adding more solute to the electrolyte.

Scrutinizing the observations, it could be presumed that there is something from the atmosphere that is promoting the electrolysis. In the next attempt the electrolyte prepared in the atmosphere was then used, and the set up was covered with a silicone stopper to prevent the contamination of the glove box. At the start there were visible signs for plating but within 30 secs, yellow colored formation engulfed the plating on the cathode. And if repeated without the silicone stopper, film turned black. In the subsequent trials, another

solute LiOH was added, argon atmosphere was changed to nitrogen and dry air, even then there were no signs of any plating.

Table 3a. Electrolysis Observations of One Third Molar LiCl in Pyridine at Room Temperature under Various Conditions

Solvent	Pyridine	Pyridine	Pyridine	Pyridine	Pyridine	Pyridine	Pyridine (exposed to air)
Solute	LiCl	LiCl	LiCl	LiCl	LiCl	LiCl	LiCl (exposed to air)
Working space	Fume Hood	Glove Bag	Glove Box	Glove Box	Glove Box	Glove Box	Glove Box
Atmosphere	Air	Argon	Argon (Improper purging)	Argon	Nitrogen	Dry Air	Argon
Plating	**Yes**	**Yes**	**Yes**	**No**	**No**	**No**	**No**

Table 3b. Electrolysis Observations of One Third Molar LiCl in Pyridine at Room Temperature under Various Conditions

Solvent	Pyridine	Pyridine (exposed to air)
Solute	LiCl	LiCl (exposed to air)
Working space	Fume Hood	Glove Box
Atmosphere	Air	Argon
Working Condition	Silicone stopper	Silicone stopper
Plating	**Yes**	**No**
Byproduct formation	Yellow Product seen near the plating on the copper electrode	Yellow Product seen near the copper electrode

These observations indicate that in that from the elements of air; nitrogen, oxygen, water, argon, carbon dioxide and other gases, something is necessary to catalyze the electrolysis. And, for high purity plating, the yellow product formed during the electrolysis must be dissipated via circulation throughout the process.

3.3 Electrolysis in Atmosphere with Additional Solute

Simultaneously, to increase the coulombic efficiency (use of lower voltages to get higher current densities) lithium tetrafluoroborate was added to LiCl solution. The solute $LiBF_4$ which is the most commonly used battery electrolyte was expected to increase the conductivity of the electrolyte. Atmospheric fume hood electrolysis did give higher current densities (~ 2.5 mAmp/cm^2, decreasing with electrolysis time) but when these films were checked for purity by ICP MS, dissociation of $LiBF_4$ was confirmed from the increasing boron content in the film (~10 %). Electrolysis of $LiBF_4$ plus LiCl in pyridine was carried out at constant voltages of 5V and 5.5V.

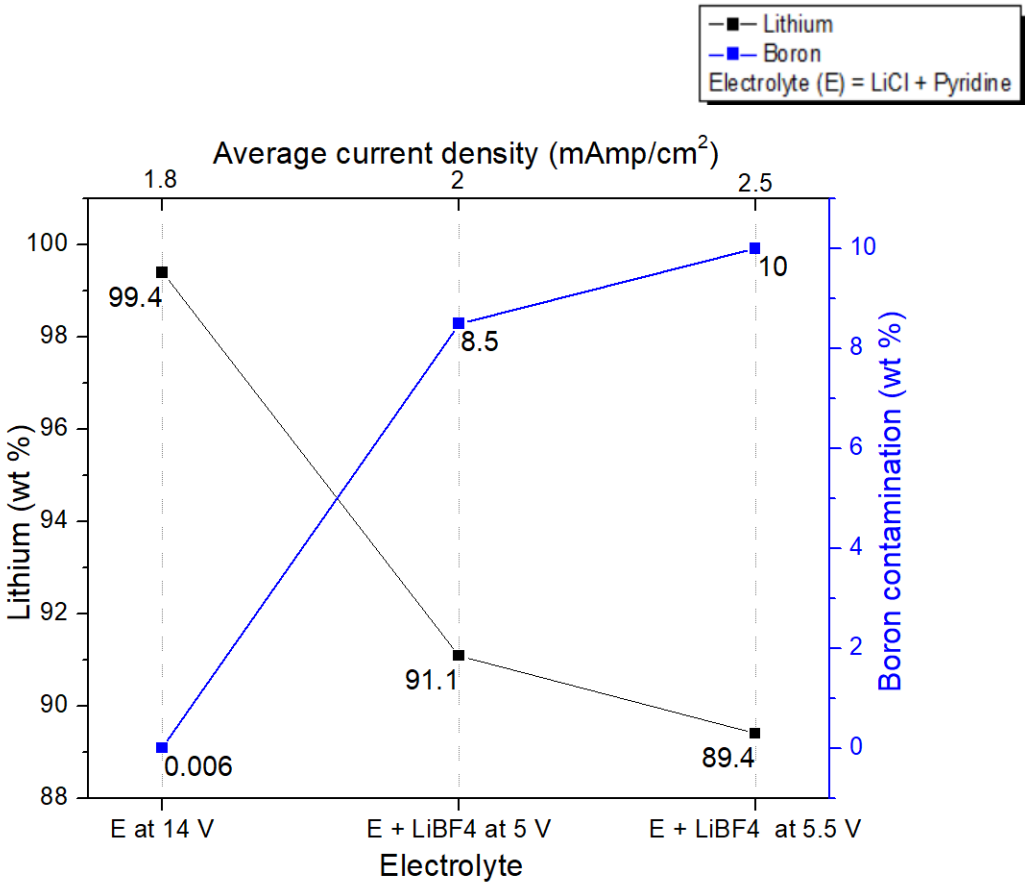

Figure 6. Weight Percentages of Li and B by ICP MS in Electroplated Films under Specified Conditions.

The lithium and boron weight percentages in the figure 6 were obtained for just 8 mins of deposition time. With such high boron content, this effort was abandoned.

3.4 Electrolysis in Controlled Atmosphere

Electrolysis was performed under specified parameters as in table 4. In the fume hood for various trials, the relative humidity (RH) varied from 22 to 26 percent depending on the daily weather conditions. In the glove box for dry air, two grades were used – Breathing grade and Ultra Zero. The lowest relative humidity in the glove box observed for Breathing Grade was 6.57 % and for ultra-zero, RH went down to 1 %. During the electrolysis it changed by a factor of 0.05. For ultra-high pure argon, the RH went down to 6.18 % even after overnight slow purging. This might be due to the earlier extensive use of glove box in air products containing moisture. Appendix A discuss oxygen content in the glove box.

Table 4. Specified Conditions for Electrolysis in Controlled Atmosphere

Air RH ~ 22 to 26 %	Ultra-high pure Argon, RH ~ 6.18 %		Dry Air, breathing grade, RH ~ 6.57 %		Dry Air, Ultra Zero, RH ~ 1.5 %	
No added water	Without water	With water	Without water	With water	Without Water	With Water

Nitrogen atmosphere was eliminated, since lithium film plated immediately turned black. Also, previous study on the macroscale reduction of LiCl in pyridine when nitrogen was used for deaeration stated the formation of red- black precipitate, potentially a mixture of lithium nitride and metallic lithium [15]. During the electrolysis of one third molar lithium chloride in pyridine at room temperature with relative humidity 22 % and 26 %, it was seen that the electroplating sustained for different time lengths before the turning black of film. It could be attributed either to different amount of moisture absorbed from the air or the

number of secondary products formed in each trial. From figure 5, at 22 % RH, the deposition lasted for 50 percent more time than 26 % RH but with lower current densities.

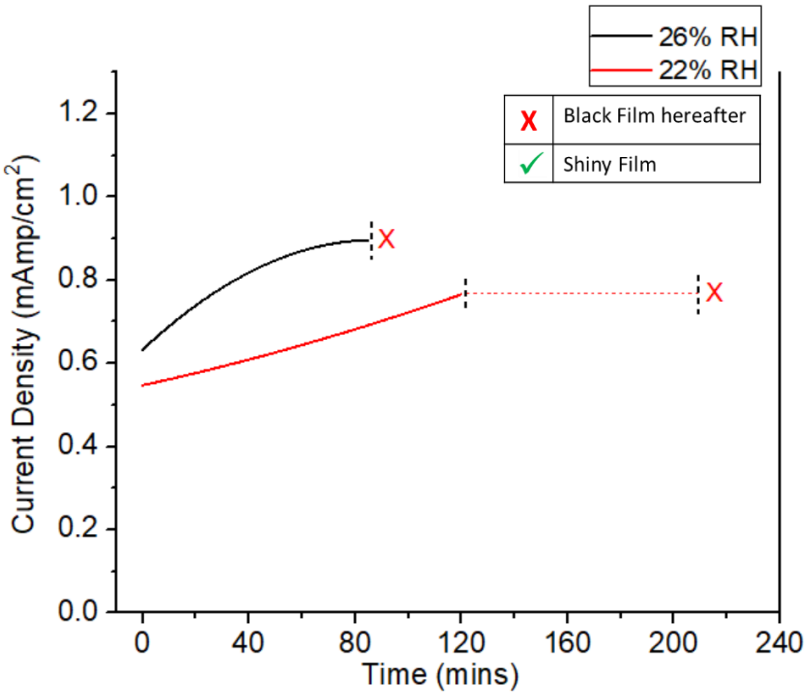

Figure 7. Current Density vs Time Graph at Different Relative Humidity (RH) Values in Atmospheric Fume Hood

Further, electrolysis was carried out in a glove box without water. Conditions and observations for the first fifteen minutes of the electrolysis have been listed in the tables below. Even after further continuation, no plating was ever seen.

Table 5. Electrolysis Parameters in Dry Air, Relative Humidity 6.57 %, without Water

Current density (mAmp/cm^2)	**Time (mins)**	**Comment**
0.5	Start	
0.403	1	No plating
0.398	2	No plating
0.395	3	No plating
0.392	5	No plating
0.624	10	No plating
0.645	15	No plating

Table 6. Electrolysis parameters in Dry Air, Relative Humidity 1.5 %, without Water

Current density (mAmp/cm^2)	**Time (mins)**	**Comment**
0.58	Start	
0.43	1	No plating
0.41	2	No plating
0.39	3	Slightly black, No plating
0.445	5	No plating
0.46	10	Yellow edges, No plating
0.48	15	No plating

Table 7. Electrolysis parameters in Argon, Relative Humidity 6.18 %, without Water

Current density (mAmp/cm^2)	**Time (mins)**	**Comment**
0.9	Start	
0.848	1	No plating
0.858	2	No plating
0.866	3	No plating
0.866	5	No plating
0.896	10	Slightly Black, No plating
1.006	15	No plating

This clearly shows that the low relative humidity existing in the glove box in an atmosphere isn't sufficient to catalyze the reaction. Hence, in the subsequent experiments, deionized water was used. If it was using water from the present RH, plating should be seen in breathing grade which had about 6.57 % relative humidity.

With the addition of 0.25 percent of deionized water, solutions of LiCl in pyridine were then electrolyzed in ultra-high pure argon and dry air – breathing grade and ultra-zero at 6 volts. The lithium deposit was smooth and had little action from the pyridine.

First the comparison was done only between dry air – breathing grade and argon atmospheres. Figure 8 shows that for the same time periods, the trial with argon had higher current densities and the film turned black. However, in the case of breathing grade, lower current densities were observed, and the film was smooth and shiny. This indicate that the

if the electrolysis was not stopped, it could be continued further to get shiny lithium. To get exact implications, instead of breathing grade, dry air ultra-zero was used.

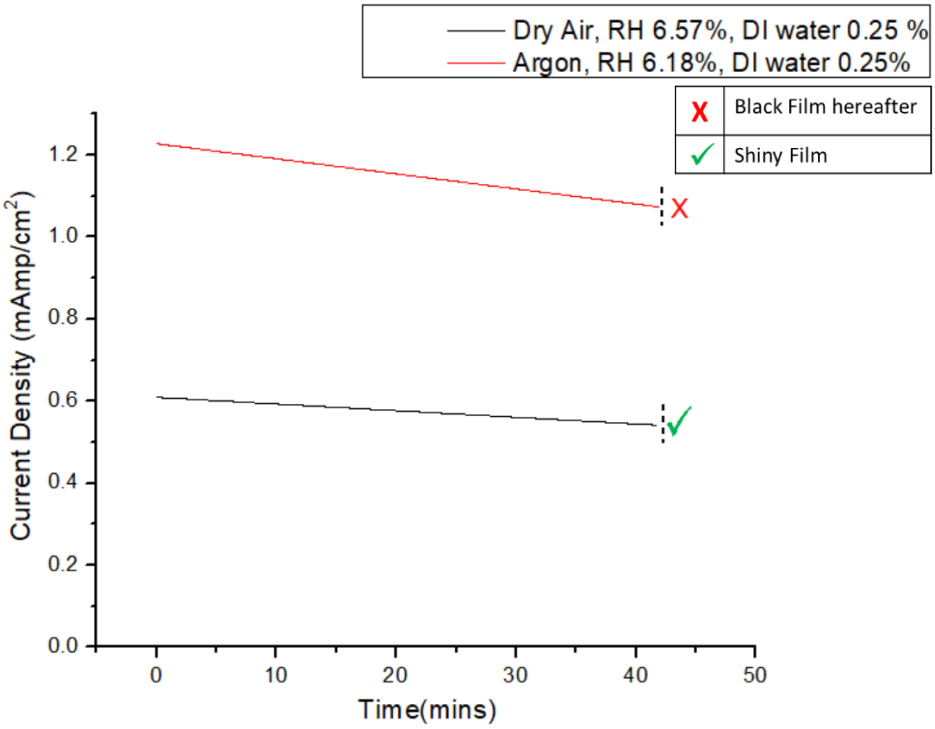

Figure 8. Current Density vs Time Graph in Dry Air and Argon with Different Relative Humidity (RH) Values on Addition of 0.25 % Deionized (DI) Water

From figure 9, shows that electrolysis under for ultra-zero and breathing grade dry air conditions, similar current densities occur. When electrolysis was further continued in ultra-zero air, it went on for seventy-eight minutes. This is almost 50 % more than that for argon, before turning black. Assumptions can be made that the secondary products formed have lowered their rate of formation by approximately 50 percent in ultra- zero dry air. But reaction kinetics does not always have direct proportionality which leads to ambiguity. This uncertainty has been further supported by the fact when the electrolysis in argon atmosphere with water content reduced to half – 0.125 % went on for more than 90 minutes without turning black.

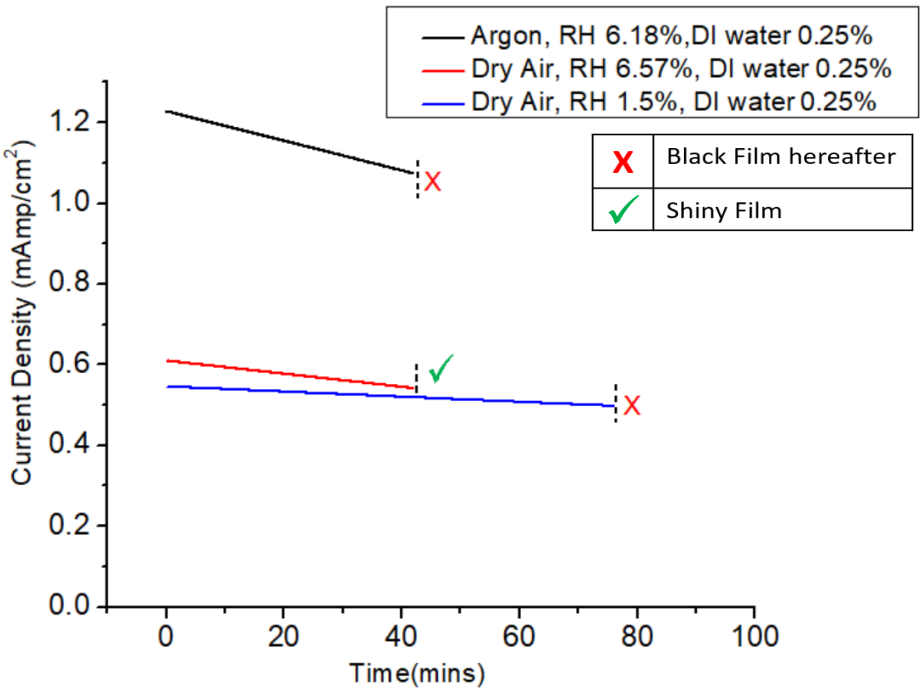

Figure 9. Current density vs Time Graph in Different Atmospheres with Different Relative Humidity (RH) Values on Addition of 0.25 % Deionized (DI) Water

We have sufficient evidence to state that the presence of water is necessary for the electroplating to occur. The next sub-chapter discuss the effect of water on pyridine.

3.5 Effect on Pyridine on Interaction with Water

Pyridine is a water-soluble liquid. From the vibrational spectroscopy of pyridine and water mixtures, the formation of hydrogen bond (HB) at the N site of pyridine and H site of water has been proposed to be a crucial step in electrolytic deposition. This HB formation was validated due to the reasonable energy peak shifts of both N and the ortho – C sites as compared to the meta- and para- C sites of pyridine [16]. The reaction is as follows

$C_5H_5N + HOH \rightarrow C_5H_5N\text{---}HOH$

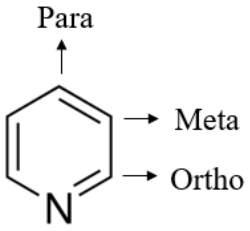

Figure 10. Ortho, Meta, Para Carbon Sites of the Pyridine Ring

The earlier study of infrared absorption of metal nitrates in pyridine and pyridine-water mixtures gives use the local structure of pyridine and water mediated pyridine ring in presence of the salts [17]. Figure 11 illustrates this structure (M = Li^+ or any metal)

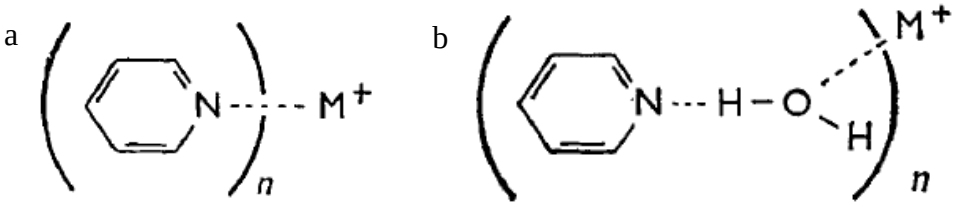

Figure 11. Structure of Pyridine in Presence of Metal Salts a) without Water b) with Water[16]

The pyridine molecules which are not hydrated form a strong metal- pyridine cation. During conditions of electron transport, electrons do not contribute to the reduction of metal. The cation complex in figure 11a preserves the ring structure and opens it only on the consequent hydrolysis when in contact with water. Earlier studies on the electrochemistry of pyridine concluded that the reduction of the solvent plays an essential role after its hydrolysis and air oxidation [16]. Elving and Cisak have discussed the structure of primary products produced during pyridine electrochemistry and the similarity of these products with the chemical reduction means. The infrared spectroscopy data of the reaction products for the electrochemical reduction of LiCl and water-pyridine solutions is comparable with this mentioned work.

One third molar solution of LiCl in pyridine was electrolyzed in atmospheric fume hood (relative humidity 22 %) at 6 V for 2 hours. The pyridine is exposed to air and hence mediated with water network. Samples for the FTIR were – pyridine, the electrolyte before electrolysis, electrolysis products after 15 mins, 30 mins, 60 mins and 120 mins.

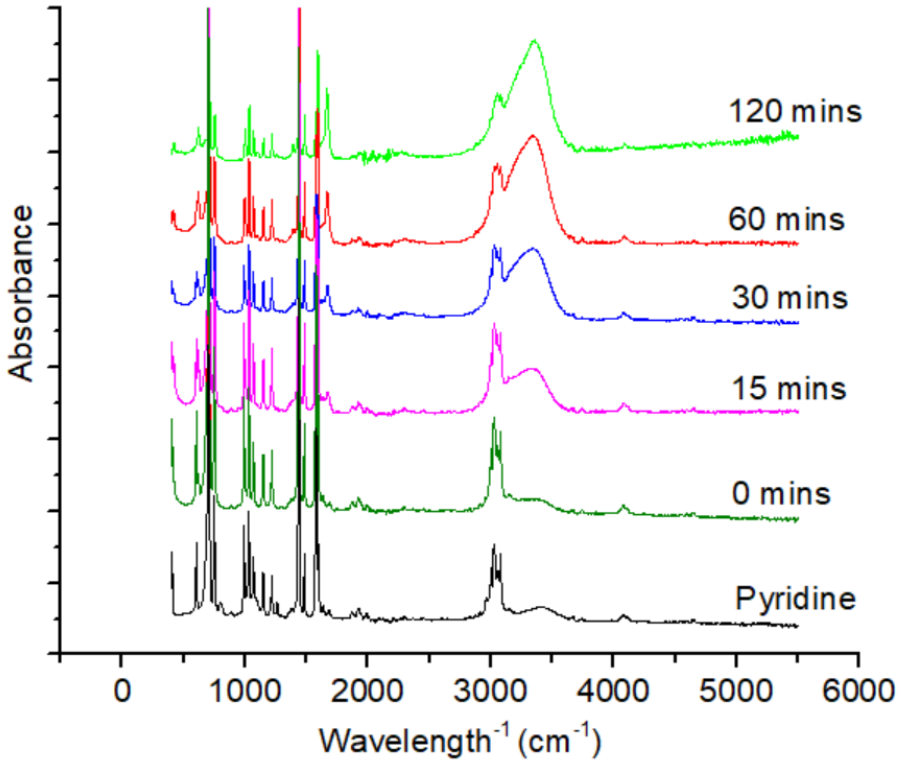

Figure 12. Infrared Spectra of Pyridine , Before Electroplating and After Electroplating at Various Time Intervals

To simplify the comparision of various spectra from figure 10, let us consider two sections a) pyridine and pyridine plus LiCl before electroplating b) electrolytic products as a function of time.

From the spectroscopy data of figure 12, the lithium chloride in pyridine posseses many characteristics of the pyridine spectra. Because of the low solubility of LiCl in pyridine, there is no appreciable associations between the solute and solvent which would cause

chemical reactions or any kind of dissociations. There are not many drastic changes except the disapperance of two peaks at 800 cm^{-1} and 1257 cm^{-1} is seen. The peak at 800 cm^{-1} represents the C-H bend (para) of aromatics. With the absence of this peak there is breaking of the pyridine ring. The data on peak 1257 cm^{-1} could not be gathered.

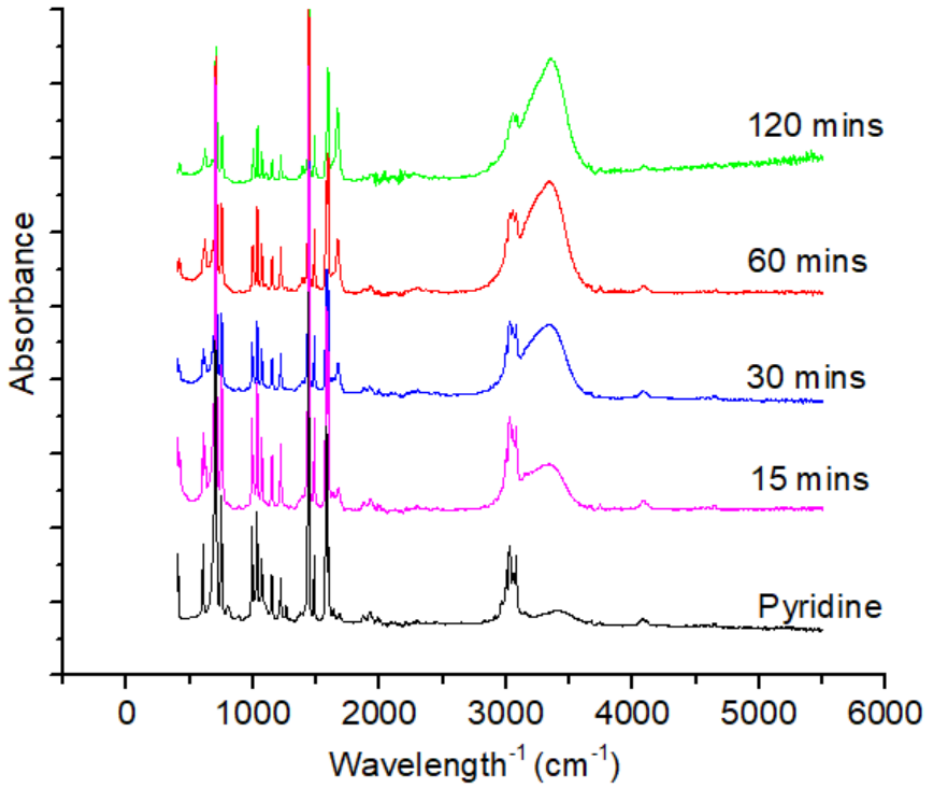

Figure 13. Infrared Spectra of Pyridine and Electrolyte at Different Time of Electrolysis

Further even in the presence of electron transport, two new peaks are clearly visible with increasing intensity at 1667 cm^{-1} and 3350 cm^{-1} .

The spectra in figure 13 represents mixtures of polyamines and polyamides. There are characterstic peaks of amines and amides from table 8 & 9 observed in the spectra. The peaks at 3000 cm^{-1} , 1450 cm^{-1}, and 710 cm^{-1} are also a representateive feature of the

polyethylene spectrum[18]. So the opening of the pyridine ring and presence of linear chains in the product is also possible.

Table 8. Characterstic IR Peaks of Amines[19]

Amines	
Peak	Frequency cm^{-1}
N-H stretch	3500-3300
N-H bend	1640-1500
C-N Stretch (alkyl)	1200-1025

Table 9. Characterstic IR Peaks of Amides[19]

Amides	
Peak	Frequency cm^{-1}
N-H stretch	3500-3080
C=O	1680-1630
N-H bend	1640-1550
N-H bend (Primary)	1570-1515

3.6 Purity of Film

For the electrolysis of one third molar LiCl in pyridine in atmosphere at 6 V for 30 mins, the lithium film was tested for purity. The lithium film was dissolved in ultra-high pure water and then acidified to 2 % HNO_3 and the method described in experimental section 2.2.2 has been followed. The detection limits were parts per billion. The ppb content of the elements was converted to mole fraction by weight and then percentage purity was calculated. The lithium weight percentage was 99.436 %. The highest impurity was contributed from the copper electrode. Sodium and potassium could have been from the lithium salt used. There is a possibility that calcium, magnesium, iron might be introduced during cleaning the beaker and other apparatus for the electrolysis. Regardless, the purity of the lithium is exceptionally high.

Table 10. Weight Percentages of Various Elements Present in the Lithium Film

Element	**Weight%**
Li	99.436
Cu	0.4140
Al	0.0412
Na	0.0348
Ca	0.0261
K	0.0174
Zn	0.0081
Fe	0.0070
P	0.0059
Mg	0.0038
Ga	0.0017
B	0.0009
Ba	0.0007
Cr	0.0005
Ni	0.0002
Sr	0.0002
Cs	0.0001
Mn	9.5E-05
Pb	9.38E-05
Ti	7.51E-05
As	4.41E-05
Mo	3.82E-05
Sb	1.78E-05
Cd	1.72E-05
W	1.7E-05
Be	1.59E-05
V	1.23E-05
Rb	8.27E-06
Zr	6.04E-06
Ce	2.73E-06
Co	1.65E-06
Eu	1.54E-06
Dy	9.16E-07
La	5.75E-07
Nd	3.75E-07
Pr	3.72E-07
Tl	2.47E-07
Hf	1.68E-07
Th	1.22E-07
U	7.21E-08

3.7 Approximate Coulombic Efficiency

The thickness of the deposited film could not be measured by any simple characterization techniques because transfer of the lithium from the working area to characterization technique chamber without exposing to air turned out to be impossible. Efforts were taken to coat the film with any inert material like titanium or nickel. For this also, the transfer was quite challenging. Two ways – first using a glove bag and second using fluorinert (FC-43 , inert solvent) were tried but lithium film somehow got oxidized. In due course, the film thickness was calculated from the mass of the copper electrode before and after electroplating. Again, this could be done only in Argon atmosphere due to the high sensitivity of lithium. Assuming this value to be similar for other conditions mentioned in table 4. The observed thickness should follow the faraday's law of electrolysis for mass of the deposited film. But since we do not have constant current density, the curve is integrated over time.

a) Calculated Thickness

   Electrolysis of one third molar LiCl in pyridine at 6 V in Argon atmosphere with 0.25 % water is carried out. The integrated curve of current density vs time gives an area of 48.3269 units. By Faraday's law of electrolysis –

   Atomic mass of lithium(m): 7, (I x t)/A = 48.33 units, density: 0.534 g/cc

   Faraday constant = 96485

   $$\text{Thickness} = \frac{m \times I \times t}{F \times d \times A}$$

   Calculated Thickness = 394 µm

b) Measured Thickness

Weight of the electrode before electroplating: 3.26 grams

Weight of the electrode after electroplating: 3.30 grams

Weight of lithium = 3.30 – 3.26 = 0.04 grams

Area: 2.56 cm^2, Density of lithium: 0.534 g/cc

$$\text{Density} = \frac{\text{Mass}}{\text{Volume}} = \frac{\text{Mass}}{\text{Area x Thickness}}$$

Measured Thickness = 29.3 μm

c) $$\text{Efficiency} = \frac{\text{Measured thickness}}{\text{Calculated thickness}} = 7.43\ \%$$

CHAPTER 4

CONCLUSIONS & FUTURE WORK

Lithium can be electroplated from a relatively cheap room temperature solution of lithium chloride in pyridine only if sufficient water is present to hydrate the pyridine. Though the low and constantly varying current densities at constant voltage do not make this the most preferable route to electroplate lithium. But looking at the purity content of the film, still a thought could be given to this process.

In future work, the water content can be optimized so that fewer secondary products are formed and the time of deposition can be increased. Also, much more work has to be done on the characterization of the film – for thickness, uniformity and most importantly purity. Trace impurities like oxygen, carbon, nitrogen, hydrogen which immediately react with lithium have to be measured.

REFERENCES

1) LITHIUM - U.S. Geological Survey, Mineral Commodity Summaries, January 2018.Retrieved from https://minerals.usgs.gov/minerals/pubs/commodity/lithium/mcs-2018-lithi.pdf

2) Albertus, P., Babinec, S., Litzelman, S., & Newman, A. (2018). Status and challenges in enabling the lithium metal electrode for high-energy and low-cost rechargeable batteries. Nature Energy, 3(1), 16.

3) Placke, T., Kloepsch, R., Dühnen, S., & Winter, M. (2017). Lithium ion, lithium metal, and alternative rechargeable battery technologies: the odyssey for high energy density. Journal of Solid-State Electrochemistry, 21(7).

4) Averill, W. A., & Olson, D. L. (1978). A review of extractive processes for lithium from ores and brines. In Lithium Needs and Resources (pp. 305-313). Pergamon.

5) Kahlenberg, L. (1899). Note on the preparation of metallic lithium. Journal of Physical Chemistry, 3(9), 602-603.

6) Patten, H. E., & Mott, W. R. (1908). Decomposition Curves of Lithium Chloride in Pyridine and in Acetone: The Effect of Water. The Journal of Physical Chemistry, 12(2), 49-74.

7) Patten, H. E., & Mott, W. R. (1904). Decomposition curves of lithium chloride in alcohols, and the electrodeposition of lithium. The Journal of Physical Chemistry, 8(3), 153-195.

8) Neudecker, B. J., Dudney, N. J., & Bates, J. B. (2000). "Lithium-free" thin-film battery with in situ plated Li anode. Journal of the Electrochemical Society, 147(2), 517-523.

9) Qian, J., Adams, B. D., Zheng, J., Xu, W., Henderson, W. A., Wang, J., ... & Zhang, J. G. (2016). Anode-free rechargeable lithium metal batteries. Advanced Functional Materials, 26(39), 7094-7102.

10) Porthault, H., & Decaux, C. (2016). Electrodeposition of lithium metal thin films and its application in all-solid-state microbatteries. Electrochimica Acta, 194, 330-337.

11) Mashtalir, O., Nguyen, M., Bodoin, E., Swonger, L., & O'Brien, S. P. (2018). High-Purity Lithium Metal Films from Aqueous Mineral Solutions. ACS Omega, 3(1), 181-187.

12) Tang, W., Yin, X., Chen, Z., Fu, W., Loh, K. P., & Zheng, G. W. (2018). Chemically polished lithium metal anode for high energy lithium metal batteries. Energy Storage Materials, 14, 289-296.

13) What is ICP MS? …and more importantly, what can it do? Retrieved from https://crustal.usgs.gov/laboratories/icpms/intro.html.

14) How FTIR spectrometer Operates Retrieved from https://chem.libretexts.org/Bookshelves/Physical_and_Theoretical_Chemistry_Textbook_Maps/Supplemental_Modules_(Physical_and_Theoretical_Chemistry)/Spectroscopy/Vibrational_Spectroscopy/Infrared_Spectroscopy/How_an_FTIR_Spectrometer_Operates.

15) Cisak, A., & Elving, P. J. (1963). Electrochemistry in Pyridine I. Polarography and Macroscale Electrolysis of Inorganic Salts. Journal of The Electrochemical Society, 110(2), 160-166.

16) Nagasaka, M., Yuzawa, H., & Kosugi, N. (2018). Intermolecular Interactions of Pyridine in Liquid Phase and Aqueous Solution Studied by Soft X-ray Absorption Spectroscopy. Zeitschrift für Physikalische Chemie, 232(5-6), 705-722.

17) Thompson, W. K. (1964). 763. A study of ammonium, lithium, silver, and pyridinium nitrates in saturated solution in pyridine and, together with potassium nitrate, in pyridine–water mixtures, by means of infrared absorption spectroscopy. Journal of the Chemical Society (Resumed), 4028-4034.

18) Cisak, A., & Elving, P. J. (1965). Electrochemistry in pyridine-IV. Chemical and electrochemical reduction of pyridine. Electrochimica Acta, 10(9), 935-946.

19) Principal IR Absorptions for Certain Functional Groups. academics.wellesley.edu/Chemistry/chem211lab/Orgo_Lab_Manual/Appendix/Instruments/InfraredSpec/Chem211%20IR%20Lit%20Value%20Table.pdf.

APPENDIX A

OXYGEN CONTENT IN THE GLOVE BOX

To determine the amount of oxygen present in the glove box after an overnight slow purge, the flow rate and the pressure readings of the cylinder were noted. Initially the glove box was under air which was purged with inert gas argon overnight at a flow rate of 20 scfh (standard cubic feet per hour). Though this flow rate is seen on the rotometer, it is later seen that this reading is suspected.

Analogous to the mixing problems, first way to determine the concentration of oxygen which is changing with time is to form a differential equation.

$$\text{Rate of change of } O2 = \text{Inflow rate of } O2 - \text{Outflow rate of } O2$$

Since argon is being purged, the inflow rate of O_2 is zero. The outflow rate is the flow rate of argon times the oxygen concentration at that time per unit volume.

$$dA/dt = 0 - \frac{A(t)^* \text{ Flow rate of argon}}{\text{Volume of the glove box}}$$

A(t): O_2 content at time t, Flow rate of argon: 20 scfh, Volume of the glove box:18 ft^3

$$dA/dt = - A(t)^* \frac{20\ ft^3/hr}{18\ ft^3} = - 1.11\ A(t)\ hr^{-1}$$

$$dA/dt + 1.11\ A(t)\ hr^{-1} = 0 \quad \ldots\ldots\ldots\ldots\ldots\ldots\ldots\ldots\ldots\ldots \quad (1)$$

Solving this first order differential equation (1)

$$\ln|A| = - 1.11\ t\ (hr) + k \quad \ldots\ldots\ldots\ldots\ldots\ldots\ldots\ldots\ldots\ldots\ldots\ldots \quad (2)$$

Solving for the value of constant k, we use

A(0) : 20% * volume of glove box = 0.2 * 18 ft^3 = 3.6 ft^3 , putting these values in equation (2)

$$\ln 3.6 = -1.11 * 0 + k$$

$$k = \ln 3.6$$

With this the equation (1) becomes

$$\ln|A| = -1.11t\ (hr) + \ln 3.6$$

Taking exponential of both sides

$$A(t) = 3.6 * \exp[-1.11t\ (hr)] \text{ …………………………… (3)}$$

Oxygen concentration per volume of the glove box is *$A(t) = 0.2 * \exp[-1.11t\ (hr)]$*

Assuming the rotometer is correct, with every exchange the oxygen content decreases by a factor of exp (1.11). The slow purge was done overnight for 18 hours, A(18) = 0.2 * exp (-19.98) = 0.42 parts per billion of the entire volume of glove box.

The same expression can give us the relative humidity values. Before purging the RH was 8.14 %. RH at time t = 8.14*exp[-1.11t (hr)]. After 18 hours, RH should be negligible.

However, the amount of argon purged into the glove box overnight was 180 psi based on the pressure readings of the argon tank. The volume of the argon tank is approximately 225 ft^3, therefore 180 psi is equivalent to 18.4 ft^3 of argon. The volume of the glove box being 18 ft^3, there was only one exchange of volume. The time period for one exchange was 18 hours. During this one exchange, the relative humidity values on the hygrometer changed from 8.14 % to 5.75 %. Under assumption of perfect mixing, the RH should decrease by a factor of 1/e, that is the RH should have been 2.99 %. Subsequently, the glove box was fast purged for 4 hours using 300 psi of argon. With this, there were two exchanges starting from 5.75 % RH. The RH should have been 0.77 %, but the RH value on the hygrometer was 0.28 %. So, this question the assumption of perfect mixing. It can be said during slow purge, there is hardly any mixing, whatever argon is flowing in is just pushing out the air.

Based on these observations, the pressure readings on the argon tank gave a more accurate amount of argon gas used, rather than the flowrate meter readings. It is possible there is a leak in the chamber, or the results could be because of incomplete mixing. It is likely, based on the pressure readings, the flowmeter did not show accurate flow rate (the ball indicating the flow rate could have been of different diameter or the density). In future to enhance the purging, the flow meter should be calibrated prior to the work and multiple exchanges should be made.